Geospatial Susceptibility Assessment of Landslide in Battagram, Khyber Pakhtunkhwa, Pakistan

Hira Shahbaz

Department of Geography, Lahore College for Women University, Lahore, Pakistan Corresponding author's e-mail: https://disable.com

Abstract

A landslide is a natural disaster that can cause significant global damage and human casualties. As a flood-prone area, the Battagram district of Khyber Pakhtunkhwa, Pakistan, has seen an increase in urbanization, making it challenging to choose an appropriate location for seismic activity. This study seeks to assess the susceptibility to landslide risk through the application such as seismic activity and flooding. This analysis employs Geographic Information System (GIS) and Remote Sensing techniques. The research utilized several data sets, encompassing geological data processed with the ArcGIS 10.8 software, Shuttle Radar Topography Mission (SRTM) data, Landsat thermal images from missions 5 and 8, thematic data, meteorological data, and a seismic catalogue. SAR photos are used to map Sentinel-1A in Google Earth Engine (GEE) to determine the extent of floods. The landslide inventory was separated into training and validation sets for this investigation. Significant contributing factors, including slope aspect, elevation, land cover and use during earthquakes, normalized difference vegetation index (NDVI), road distance, fault distance, rainfall, and geology, are taken into consideration when assessing landslip susceptibility. To establish the spatial correlation between landslides and these parameters, the frequency ratio model and weighted sum analysis were utilized. The WSM analysis indicates that 1.74% of the region is classified as having very low susceptibility, with the remaining areas being classified as low (14.26%), moderate (36.01%), high (2.57%), and very high (5.41%). 44.67% of the region is classified as having very high susceptibility by the FR model, with high (40.94%), moderate (11.61%), low (1.96%), and very low (0.79%) following. The FR model demonstrated reliability in risk assessment, with an accuracy of 85.7% against known landslide events. These findings support the use of GIS-based statistical modeling in urban planning and hazard mitigation by demonstrating how well it can identify high-risk areas. For increased accuracy and scalability, future developments should concentrate on adding more localized data.

Keywords: Landslide susceptibility, weighted sum analysis, GIS, frequency ratio, remote sensing, Google earth engine

Introduction

One of the most common geological disasters, landslides are said to cause significant property loss and fatalities all over the world (Linkha, 2024). According to CRED, the landslides segment accounts for 17% of fatalities in all natural disasters worldwide (Alimonti & Mariani, 2024). Climate models project that the intensity of monsoon rainfall in southern Asia will rise in the future owed to climate change. This could feasibly enhance the winter rebound and cause more seismic events. Rainfall and flash floods can cause rockfalls and debris flow, and environmental factors like rock deterioration over time can also cause landslides. Similarly, natural disasters like earthquakes can cause a slope to become weak due to construction along its banks (Shabbir et al., 2023). Every year, during the monsoon season, landslides and floods in the Himalayan region reason fatalities and damage to property (Sana et al., 2024). The rough terrain, active seismicity, monsoon rains, and human activity on uneven slopes make northern Pakistan one of the most landslide-prone areas (Hussain et al., 2023). The deadliest and worst flood disaster in the past ten years occurred in Pakistan in 2022. Pakistan encountered a monsoon climate and extremely hot weather in mid-June 2022 (NASA, 2022), and as a result, at least two-thirds of the nation experienced the most precipitation in almost 30 years. Following the flood in 2022, some of the highland's volcanic mountains are still active. Additionally, fissures and cracks truncate the main rock types in this highland.

Many landslides have occurred in the area as a result of earthquakes destroying them (Sana et al., 2024). In order to forecast future landslides, it is vital to identify the zones that are vulnerable. By using scientific analysis to identify and forecast landslide-prone areas, appropriate preventative measures can reduce landslide damage (Jena et al., 2021). Therefore, the two main causes of landslides in the region are earthquakes and rainfall (Vasil Levski & Dolchinkov, 2024). Using the data that is currently available and geospatial techniques, this study attempts to create landslide susceptibility mapping over the Battagram district that is caused by earthquake and flood activity. As a result, the study evaluates the primary causes of landslides in the Battagram district as well as the effects of land cover change over the previous 16 years on landslides in the study area. The study area has a primarily monsoonal climate, and landslides are typically caused by heavy rainfall. The risk of landslides is influenced by human activity in addition to climate and geotectonic factors.

Disasters appear on the news headlines almost every day, according to (Dietrich et al., 2024). Most of them take place in distant areas and pass by swiftly. In light of (Lu et al., 2024), there have been eighteen fatal earthquakes worldwide between 1989 and 2015, which have caused extensive landslides across a

wide area. Examples of large-magnitude earthquakes in the past ten years, according to (Saima Akbar, 2024), include the 2005 earthquake in Kashmir caused thousands of landslides in northern Pakistan, resulting in a thousand deaths. Some of the most notable landslide disasters that have occurred in northern Pakistan include the 2005 Kashmir earthquake, which caused thousands of landslides over an area of more than 7,500 km³ in Kashmir and its surroundings, killing 87,350 people. (Bali et al., 2025) stated that three major mountain ranges, the Himalayas, Karakoram, and the Hindu Kush, are the dominant feature of the northern regions of Pakistan. These mountain ranges comprise the world's steepest peaks with a 45° slope (Ahmed et al., 2019). Flash floods and landslides occurred on October 3-4 in Khyber Pakhtunkhwa Province (Northern Pakistan) due to heavy rain, leading to casualties. Across Charsadda and Lower Kohistan Districts, the Provincial Disaster Management Authority (PDMA) reports that two people have died and six have been injured. Rescue operations are taking place in Charsadda, as a few families have been relocated to relief camps. On October 6-7, there is a forecast of dry conditions over Khyber Pakhtunkhwa Province. Pakistan's history has shown numerous flood events starting from its creation, such as the floods of 1950, 1992, 1998, and 2010 (Saima Akbar, 2024)

Several revisions in this area focused on geospatial and GIS-based methods to analyze numerous spatial data types, the evolution of geostatistical models, and the predictable points of risk and vulnerability for a given area (Rehman et al., 2022) A susceptibility map that identifies areas that are likely to experience landslides in the future (Tyagi et al., 2023). An essential first step in hazard and risk assessment, landslide susceptibility assessment is a widespread practice worldwide, primarily utilized for landslide mitigation strategies. Landslide susceptibility assessment requires the use of remote sensing and Geospatial-derived outcomes, such as landslide inventory and contributing and triggering factors. Landslide susceptibility assessment methods can be divided into two categories: quantitative methods, such as statistical models, heuristics (multi-criteria analysis), and physical-based models, and qualitative methods, such as knowledge-based and geomorphological mapping (Batar & Watanabe, 2021). According to (Dou et al., 2019) usually, rainfall or earthquakes cause landslides, though sometimes an earthquake causes a rainfall event, or vice versa. A digital elevation model (DEM) is used in large-scale physically based landslide susceptibility processes to describe the terrain constraints that fundamentally define the local elevation, slope, hydrologic, and further geomorphic processes (Schlögel et al., 2018). Land use and land cover variation can modify the geological circumstances and distress the manifestation of the landslides (Chen et al., 2019). Remote sensing data, land-based data, and numerous other data sources are used to

extract the spatial information related to the aforementioned factors. Landslide susceptibility maps demonstrate the comparative possibility of future landslides based exclusively on the vital assets of a background or site (Rahim et al., 2018). Landslide susceptibility mapping (LSM) is regarded as a prime phase in the execution of instant disaster management planning and risk mitigation events (Camilo et al., 2017).

The occurrence of landslides is primarily ascribed to the combined effect of various factors, and it is never easy for researchers to assess the extent of these factors' influence (Abdı et al., 2021). Unusually, in recent years, firm changes in global climatic conditions have controlled to extreme weather events that increase the propensity of landslides (Zou et al., 2021). Even though landslides have been studied extensively, little is known about how floods and seismic activity interact to cause landslides. This is especially true in Northern Pakistan's Battagramdistrict, which is particularly vulnerable because of its complicated topography, active tectonics, and unpredictable climate. Current models frequently ignore the compounding effects of multiple hazards and only take into account landslide triggers in isolation. Additionally, little research has been done to incorporate changes in land cover over the past few decades into susceptibility assessments. By using the Frequency Ratio (FR) model and Geospatial techniques to generate an extensive Landslide Susceptibility Map (LSM), this study seeks to close these gaps.

Study Area

The geographical location of District Battagram is latitude 34.79147 and longitude 73.121641, which covers an area of 350,172 acres. The district usually has dense forests and mountains with peaks higher than 4000 meters. It is bordered to the north by Kohistan District, to the east by Mansehra District, to the south by the Kala Dhaka Tribal Area, and to the west

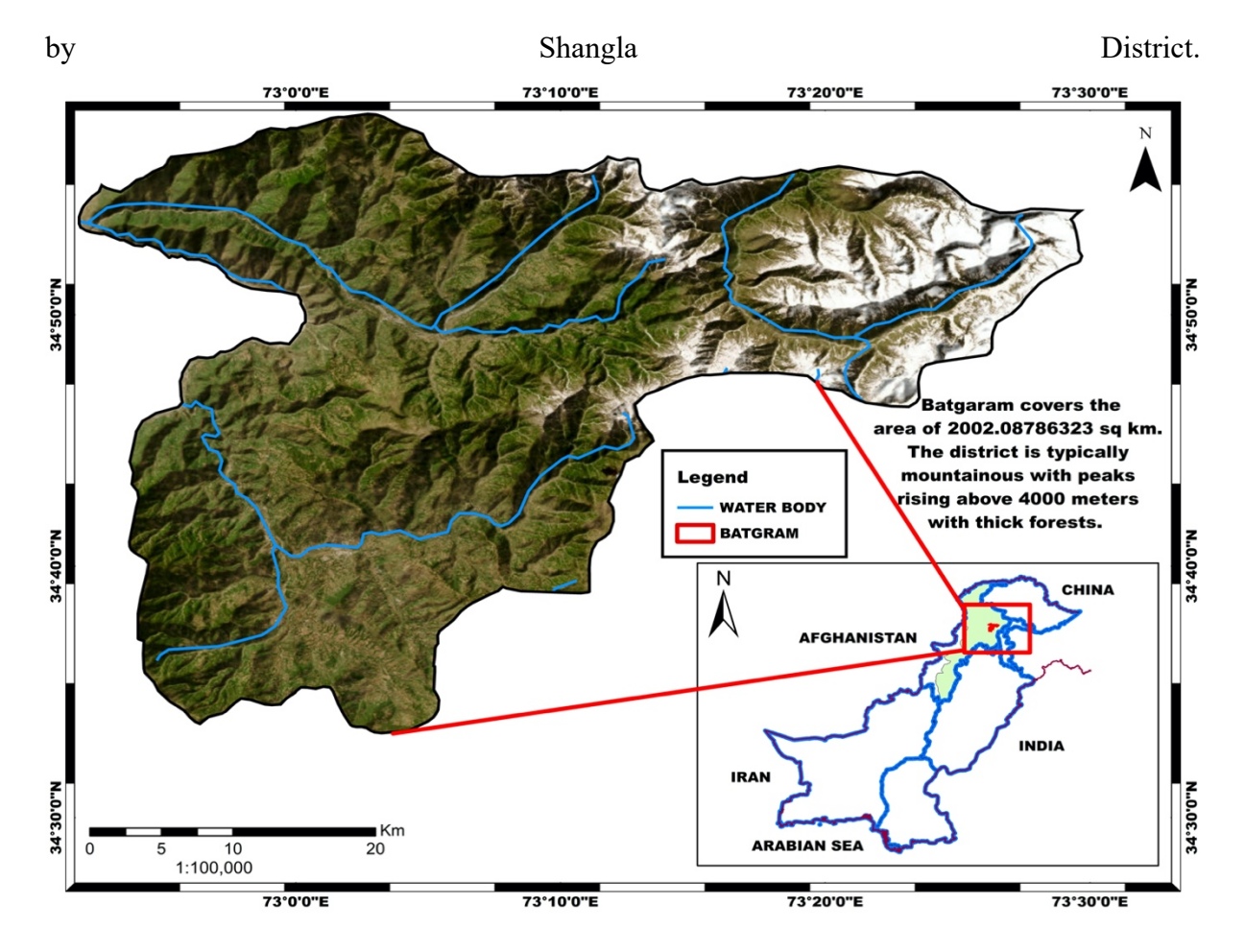


Figure 1: Study Area Map

The corporate headquarters is located in Battagram town, which is about 75 kilometers from Mansehra along the Silk Highway. Battagram and Allai are the two tehsils that make up the district. It features a number of stunning valleys. The Nindhyarkhawar and Allai Khawar are the two main streams, which are referred to as Khawar in the local dialect. Beginning in the "Hill" mountains, the Nindhyar Khawar flows over the main village before joining the Indus River at Thakot in the east. The Chaur Mountains are the source of the other large stream, Allai Khawar, which empties into the Indus River at Kund in the east. The maximum temperature on an average day for each month in Battagram is displayed by the "mean daily maximum" (solid red line). Similarly, the average minimum temperature is displayed by the "mean daily minimum" (solid blue line). The average of each month's hottest day and coldest night over the previous 30 years is displayed by hot days and cold nights (dashed red and blue lines).

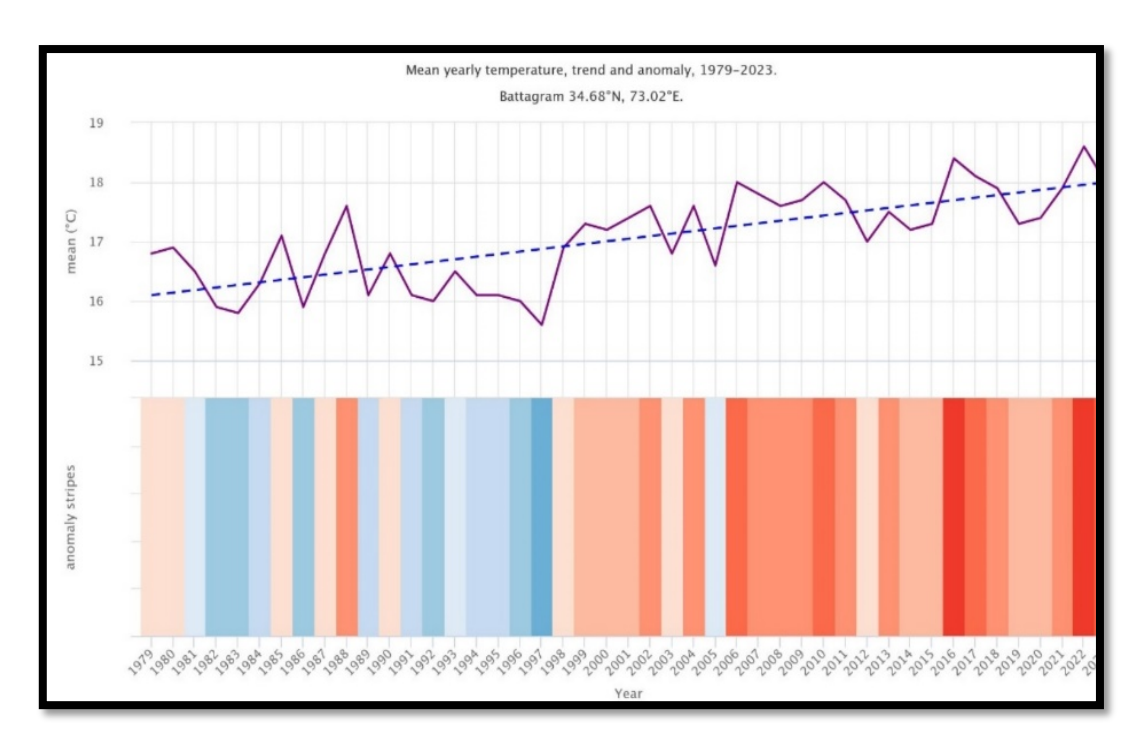


Figure 2: Graphical representation of temperature (1979) 2023)

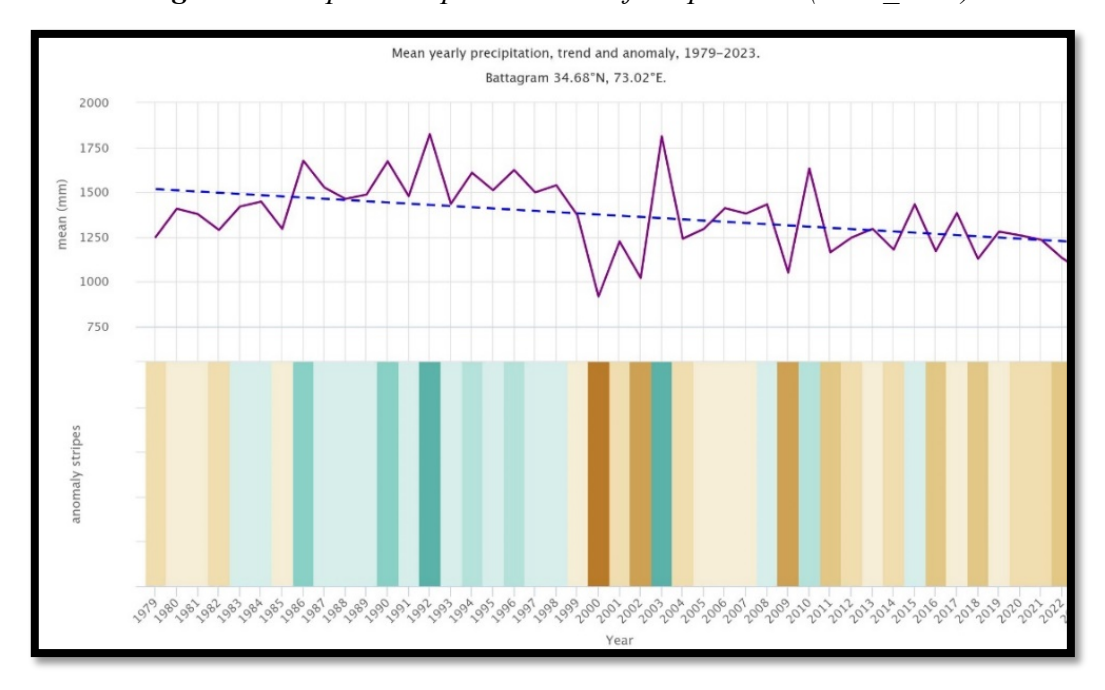


Figure 3: Graphical representation of precipitation (1979-2023)

The graph displays an approximation of the mean total precipitation for the greater area of Battagram. The dashed blue line is the linear climate change inclination. In the lower part, the graph demonstrates the so-called precipitation stripes. Respectively colored stripe represents the total precipitation of a year - green for wetter and brown for drier years. There is an entire 369 km road network in the valleys. The Karakoram Highway or the Silk Highway, arrives in the district at Sharkool, Mansehra, and leaves it at Thakot. The major roads in the

district are Battagram-shamlai, Batagram-Oghi, Battagram-paimal Sharif and Chattar-Kuzabanda road.

It's interesting to note that geologists have long recognized a connection between seismic activity and rainfall rates. For instance, the yearly rainfall cycle of the summer monsoon season in the Himalayas affects the frequency of earthquakes (Mir et al., 2024). According to investigation, only 16% of Himalayan earthquakes happen throughout the monsoon season, with 48% occurring during the drier pre-monsoon months of March, April, and May. (Munir et al., 2021) stated that Pakistan continues to experience flooding and landslides due to the country's heavy rainfall, which also causes an increasing amount of damage and fatalities. In Khyber Pakhtunkhwa Province, flash floods and landslides caused at least 13 fatalities and 27 injuries between August 31 and September 1. According to the NDMA report, there have been 2,245 damaged homes, 189 fatalities, and 128 injuries since the start of the monsoon season. According to (Bahram & R. Paradise, 2020), nearly every element of the people's socioeconomic lives as well as the district's physical infrastructure was impacted by the earthquake. In the last ten years, 1389 earthquakes of magnitude four or higher have occurred within 300 kilometers (186 miles) of Battagram, Khyber Pakhtunkhwa. This translates to an average of 11 earthquakes per month, or 138 earthquakes annually. Near Battagram, an earthquake occurs approximately every two days on average. Battagram has experienced 19 earthquakes with magnitudes greater than 2 and up to 5.0 since 2022.

Materials and Methods

Data acquisition

Multi-source data has been used for landslide susceptibility monitoring in Battagram. This study's landslide susceptibility map was created using ten factors. The factors were entirely chosen based on their availability and efficacy. For LULC variation analysis, multi-temporal cloud-free Landsat 5 and 8 Thematic Mapper (TM) data of August 2010, 2015, and 2022 (Table 1) were obtained from USGS Earth Explorer (EarthExplorer (usgs.gov). The extraction of topographic information, including elevation, slope, aspect, hill shade hydrology, was obtained from the Shuttle Radar Topography Mission-Digital Elevation Model (SRTM-DEM) with 30 m resolution. The geological data were obtained from toposheets from the Geological Survey of Pakistan (GSP) and satellite data from the U.S. Army KMZ. The monthly rainfall data from 2010 to 2022 were collected from the Data Access Viewer-NASA POWER

(https://power.larc.nasa.gov/data-access-viewer/). The historical landslide data have been collected from the NASA Landslide Viewer.

Satellite	Dates of Images	Resolution	Reference
			system/Path/Row
Landsat 5	18/06/2010	30m	WRS/150/36
Landsat 8	15/06/2015	30m	WRS/150/36
Landsat 9	20/06/2022	30m	WRS/151/40

Data processing

The data was then imported, processed, and analysed in ArcGIS software to create various maps of the factors impacting the incidence and spreading of groundwater in the watershed. Multiple factors have been considered to regulate landslide-susceptible zones.

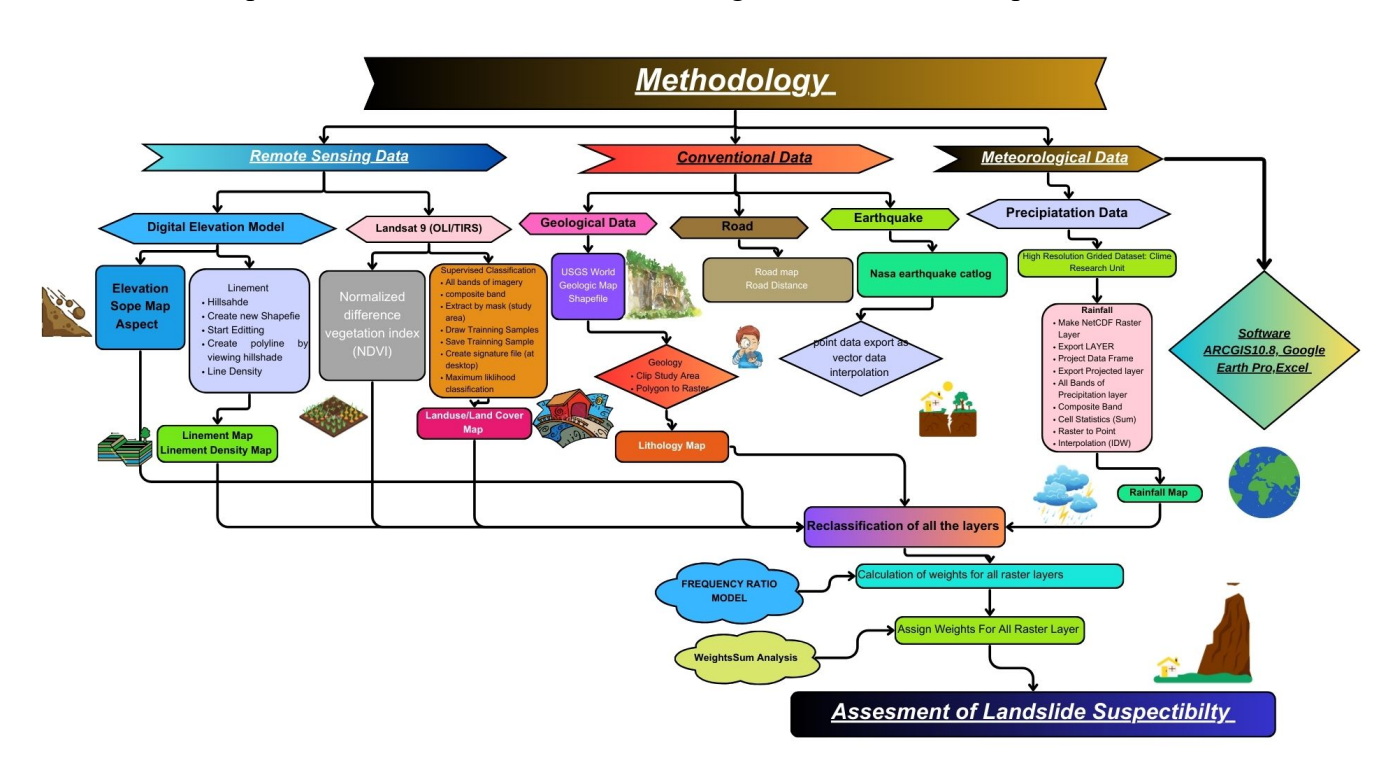


Figure 4: The methodological framework

Data analysis

Flood extent

Sentinel-1 SAR data were principally utilised in this study to map the flood inundation in the Battgaram District in 2022. A population dataset and land use/cover (LULC) have been used in the evaluation of flood damage. The Global Human Settlement Layers (GHSLs) and Gridded Population of the World (GPW v4) datasets were analyzed for population and density, respectively, in order to assess the effects of flooding. Using the monthly precipitation data from Terra Climate, the rainfall pattern and anomaly during the 2022 flood event have been recognized. The crop land and population density had been calculated using ArcGIS software.

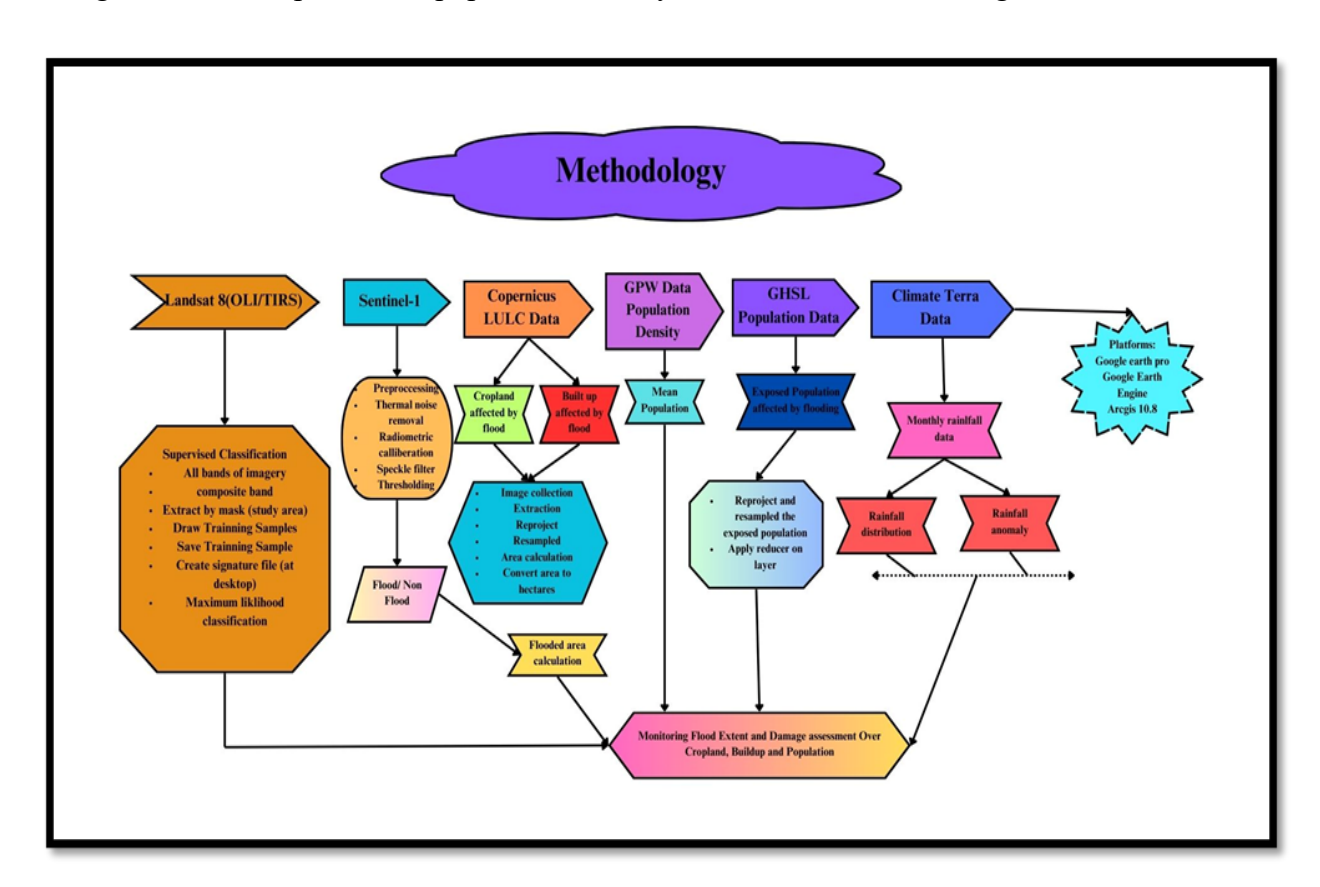


Figure 5: The methodological framework for assessment of flood extent

Landslide inventory map

A landslide inventory map, which illustrates the positions and contours of landslides, expresses the knowledge of landslides in a specific area. A data set that may include one or more incidents is called a landslide inventory. Forecasting the likelihood of landslides in a study area primarily relies on historical and present landslide inventory data. Sentinel-1 and Google Earth pictures were used to generate the landslide inventory map for this study.

Common factors controlling landslides

The primary determinants of seismic landslides include geological, seismic, and topographic factors. Ten common landslide-causative characteristics that are used to analyze landslides triggered by earthquakes and rainfall were examined in this study. The topography, geology, tectonic features, weather, land cover, and human activity all have a significant influence on the intensity and spatial distribution of landslides. It is crucial to assess how these causal elements affect the landslide's spatial distribution for the purpose to comprehend how they work and create a map of landslide vulnerability. The primary factor influencing the location and severity of landslides is the slope of the terrain (Jin et al., 2024).

Slope is an important causal component in landslide inquiry, according to (Mir et al., 2024), since it causes loose sediment material to migrate downslope. The current research area's slope was calculated using a DEM with a spatial resolution of 12.5 m. Next, using ArcGIS 10.8, the computed slope was divided into five classes, as Figure 8 illustrates. The research area's terrain aspect was calculated using a 3*3 moving window in ArcGIS 10.8 based on the DEM. It is usually recognized that lithological structures have a substantial influence on the physical potentials of both surface and subsurface material, counting their strength and permeability, which in turn influences the probability of landslides (Khan et al., 2019). The distribution of landslides is greatly affected by land cover; generally, landslides are less common in forested areas than in barren ones. Strong root systems of the vegetation give the mechanical and hydrological forces that frequently stabilize the slopes. The area's land cover was categorized as consisting of permanent snow, glaciers, irrigated agricultural land, barren ground, woodland and shrub land, and water bodies. The prevalence and intensity of co-seismic landslides are primarily determined by the spatial spreading and character of fault lines (Duan et al., 2023). The region's fault lines were taken from the geological map of the region. Using ArcGIS 10.8 software, the distance to the fault was split into five regions spaced 50 meters apart (Fig. 6e). Building roads and railroads as part of a communication network in hilly areas frequently causes instability in slopes and ultimately landslides (Dahiya et al., 2025). The road network was derived from the obtained Sentinel 1 pictures and then verified in the field to evaluate the influence of the road network on the landslides in the research area. Then, using ArcGIS software, distance from the road was measured at 50-meter intervals. Streams can cause undercutting from toe erosion and saturation of the slide toe from increased water penetration, both of which can negatively impact a slope's steadiness (Hussen et al., 2024). Using Arc Hydro tools, the stream network for the study area was computed using the ASTER

DEM to evaluate the influence of the streams on the distribution of landslides. The streams that accumulated more than 20 square kilometers were extracted.

Weighted Sum Analysis

There are ten elements - Roads, Streams, Vegetation, and Slope - and three criteria established for each element to regulate habitat correctness for the black bears. Feature to Raster, Euclidean Distance, Slope, Reclassify and Weighted sum are cast-off for the analysis. First, layers are converted and analysed to formulate for reclassification. Next, converted and evaluated layers are reclassified giving to the criteria provided in the study. Reclassification for additional specifics concerning reclassification. Finally, all the reclassified layers are draped. A map representing appropriate areas for the black bears, representing three levels of habitat suitability, is fashioned.

Frequency Ratio model

According to (Khan et al., 2019) to assess the likelihood of landslides, it is crucial to comprehend the physical features unique to the place and the mechanisms that cause them. A quantitative method for assessing landslide susceptibility that makes use of geographic data and GIS technology is the frequency ratio. For mapping landslide susceptibility, the frequency ratio (FR) technique is widely and successfully employed. It depends on the measured correlation between the causal variables for landslides and the landslide inventory. We compute the FR for each factor using Eq. 5.

FR = (Ni P x/N)/N i l Q/Nl

Where N is the total number of pixels in the study area, N i lP is the number of landslide pixels in each landslide conditioning factor, Nl is the total number of landslide pixels in the study area, FR is the frequency ratio, and Ni Px is the number of pixels in each landslide conditioning factor class.

Landslide susceptibility mapping

It is crucial to make the assumptions that future landslides will occur within the same conditions as prior landslides and that the geographical distribution of landslides is inclined by the elements that trigger landslides while doing landslide susceptibility mapping. Frequency Ratio (FR) has been utilized throughout this research to map the vulnerability to landslides.

Results and Discussion

Although landslide growth is influenced by a variety of natural and man-made elements, it is a complex process. (Khan et al., 2019). The most significant criteria for precipitation and the detachment to the fault lines were determined to be those created by consulting experts in the landslide susceptibility study (Konurhan et al., 2023). In order to lessen the effects of present and future hazards, LSM was created in this work using geospatial approaches that consider landslide events and risk influences (elevation, slope, aspect, curvature, precipitation, LULC, distance to fault, lithology, distance to road, and distance to streams).

Landslide inventory map

First, we used data from satellites and ground stations to create an inventory map. The determining characteristics for landslides can be observed in the topographic aspects of aspect, curvature, slope, and altitude. As seen in Figure 1, 324 past and present landslide occurrences in the research area were found using ground-based data and satellite imagery.

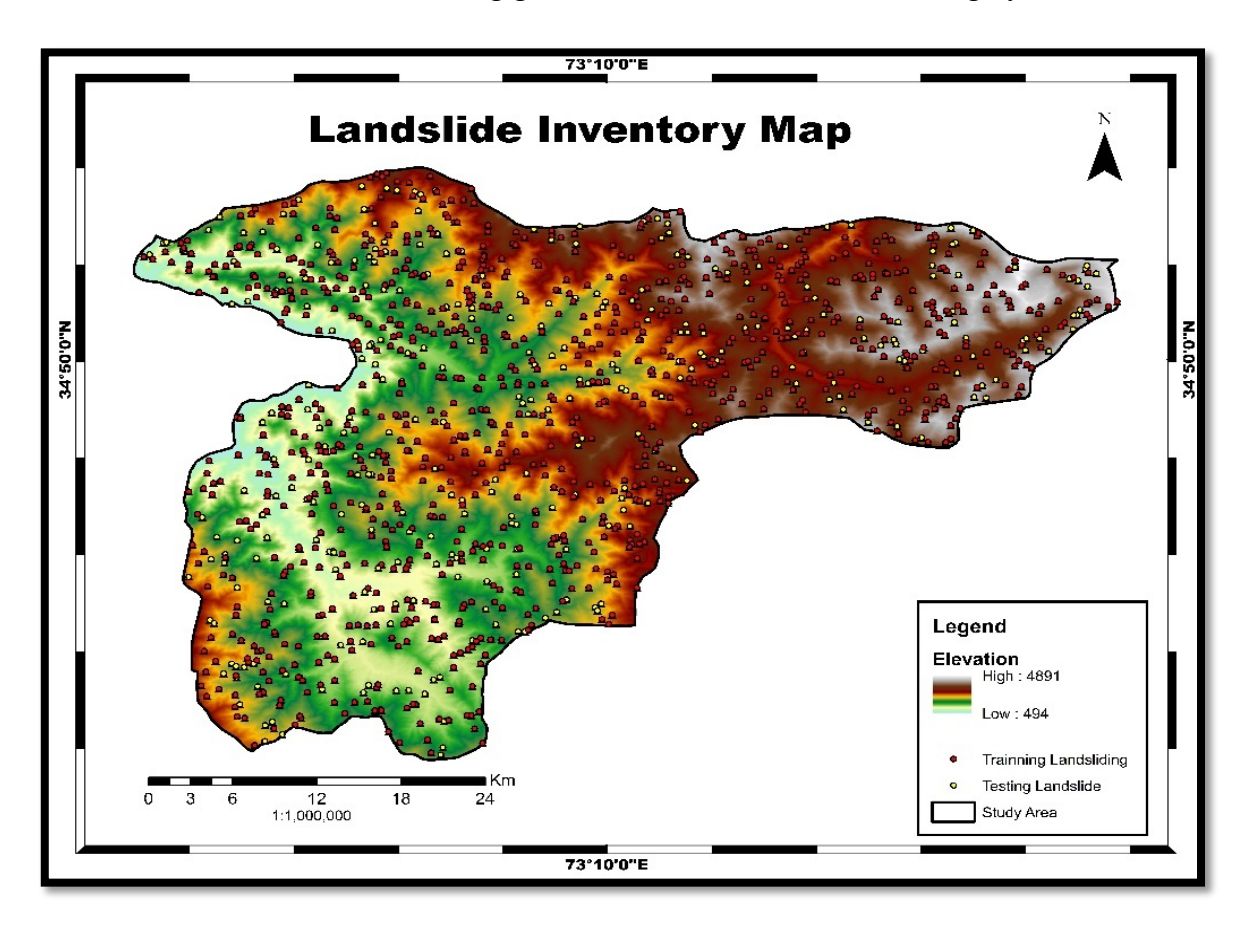


Figure 6: The landslide inventory map of Battgaram

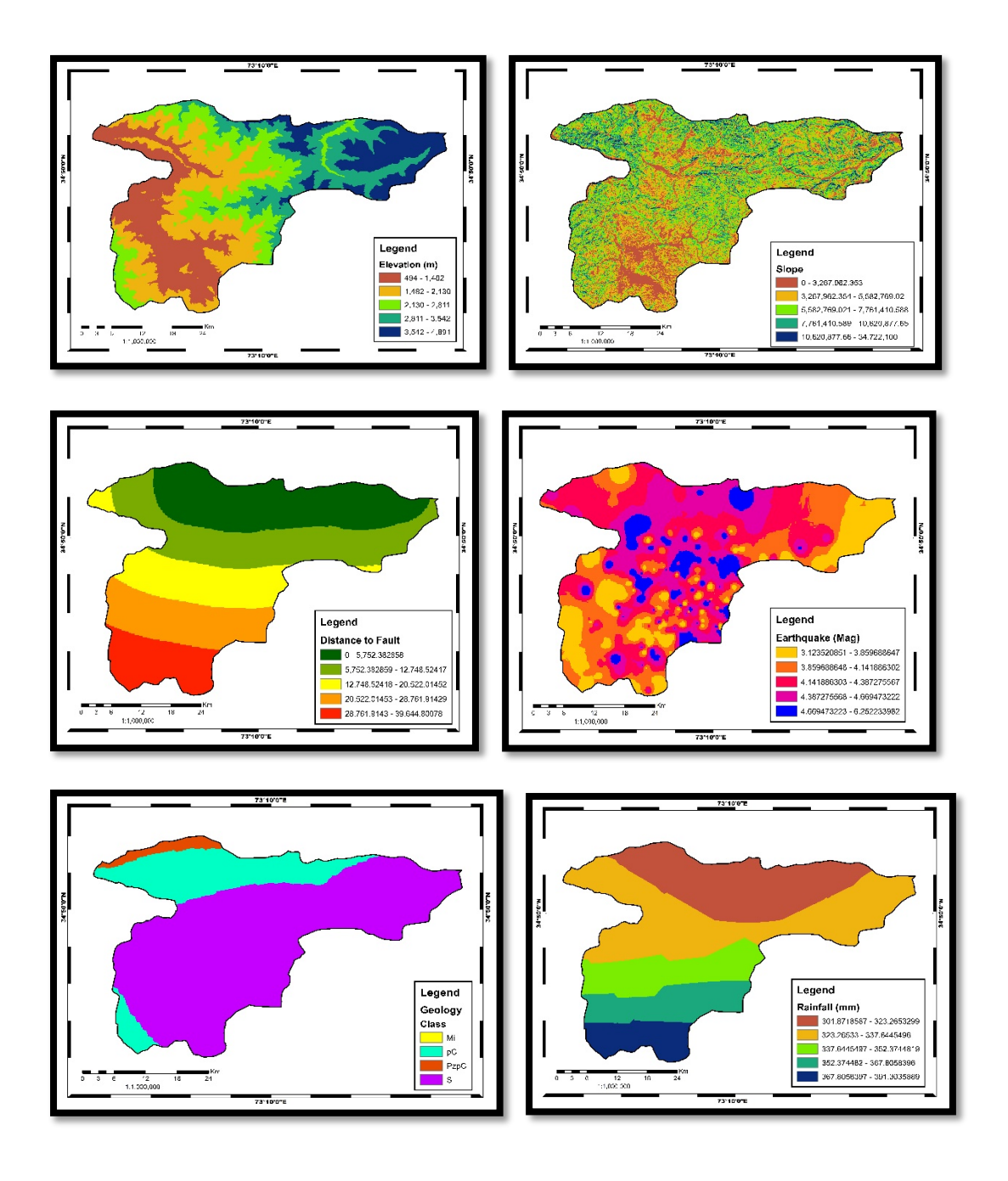
To generate a non-landslide area, we first abstract the landslide polygon after the research area polygon. Next, we created random spots in the study zone which has been designated as a non-landslide area using ArcGIS tools(Jin et al., 2024). The various forms of landslides that occur during these occurrences include mudflows, debris flows, rockfalls, and rockslides, topples, and creeps. Three bivariate models are used in this study to generate the study area's LSM. Table 2 displays particular details of each model's outcomes.

Causative Factors of Land sliding

According to (Khan et al., 2019), elevation is a significant requirement for landslide incidence. The current study's elevation characteristics show a substantial correlation with landslide occurrences. >4,500 m is the most significant elevation class, followed by 494 – 4,891 m. The slope, which is the independent variable in this study, is seen to be the most important component. According to Table 2, the slope component has an impact up to 30° because landslides occur more frequently at higher slopes. Above that point, however, landslide activity declines as the slope increases. The results showed that the most prone class of slope is 15-30 $^{\circ}$, while the most resistant class to landslides is >30 $^{\circ}$, followed by the 10 $^{\circ}$ -15 $^{\circ}$ class. According to Table 2, the most important class of aspects is SE, which E, S, and SW. As shown in Table 2, the tabulated findings clarified that the critical class of landslides is concave structure. As Table 2 illustrates, the current study's findings suggest that faults have no direct bearing on the likelihood of landslides. The findings show that a relatively limited number of landslide pixel values of 0-39,644 for WOE and FR, respectively, occurred in a zone <50 m equidistance from the fault. To measure the relationship between rainfall parameters and landslide incidents, a rainfall map derived from CHIRPS data was created in the current study, verified using data collected from the ground, and classed into five classes. The precipitation data in Table 2 indicate that rainfall plays a substantial part in the occurrence of landslides.

The precipitation period is the censorious class for landslides, according to the results, followed by 301.87–391.30 mm/year. The vegetation cover is crucial for stabilizing slopes because roots anchor and strengthen soil layers. The NDVI values of plant formations are mainly positive and fall between 0.571 to 0.086. The results demonstrate that lithology plays a major causal role in the analysis of landslides. The furthermost prone geological creation for landslides is pC, tracked by Mi, PzpC, and S, as Figure 9 illustrates. It is believed that road construction is a direct effect of human activity, which leads to slope instability. The road network map is a polyline vector generated from the data, as seen in Figure 9. As a result,

varying land use plays a vital role in determining landslide susceptibility in numerous studies (Abdı et al., 2021). Different land uses have varying effects on landslides. Table 1 results indicate that the current study area's flooded vegetation and forest land make it particularly vulnerable to landslides.



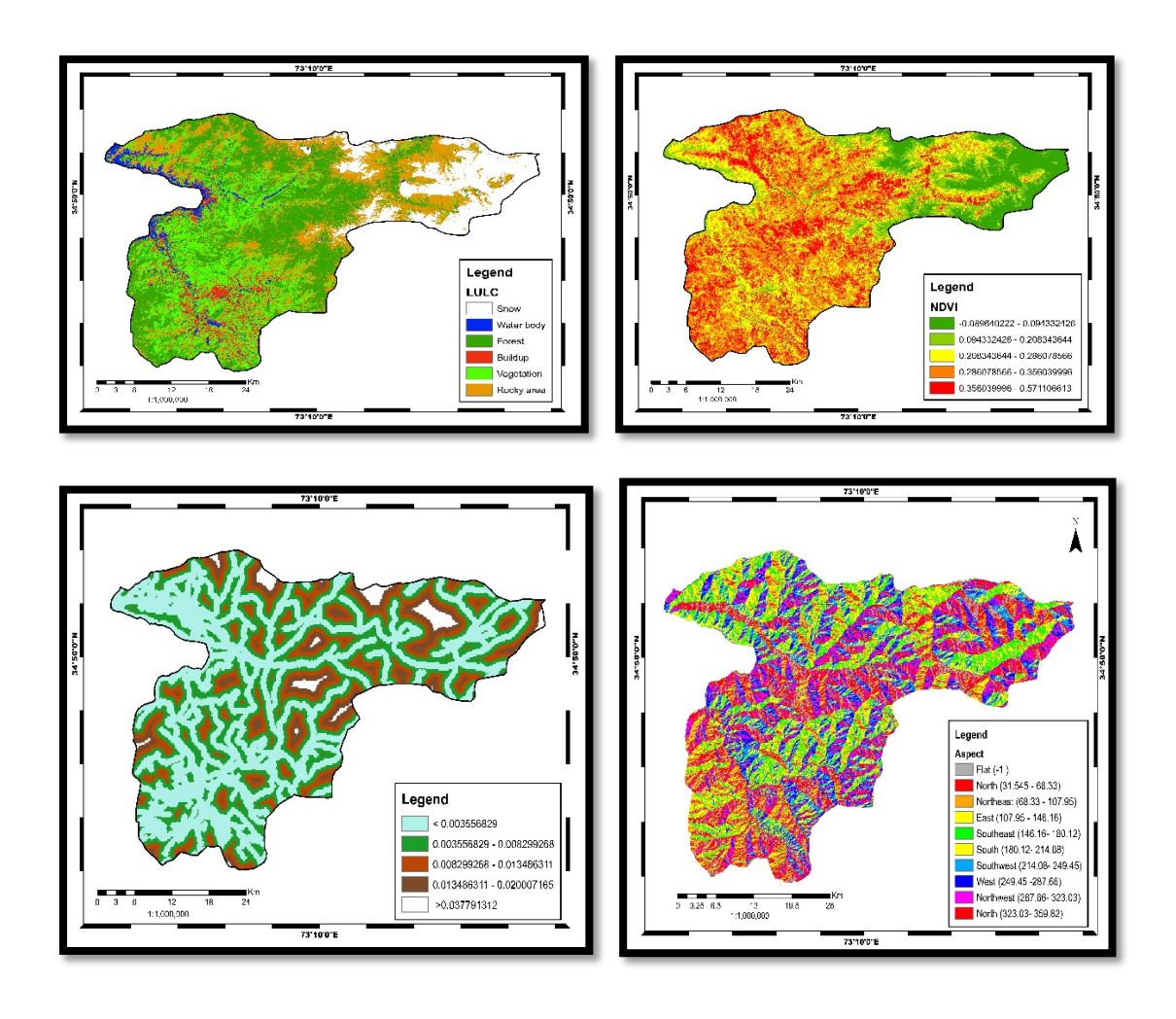


Figure 7: The resultant maps included land use and cover, geology, rainfall, lineament density, slope, and soil.

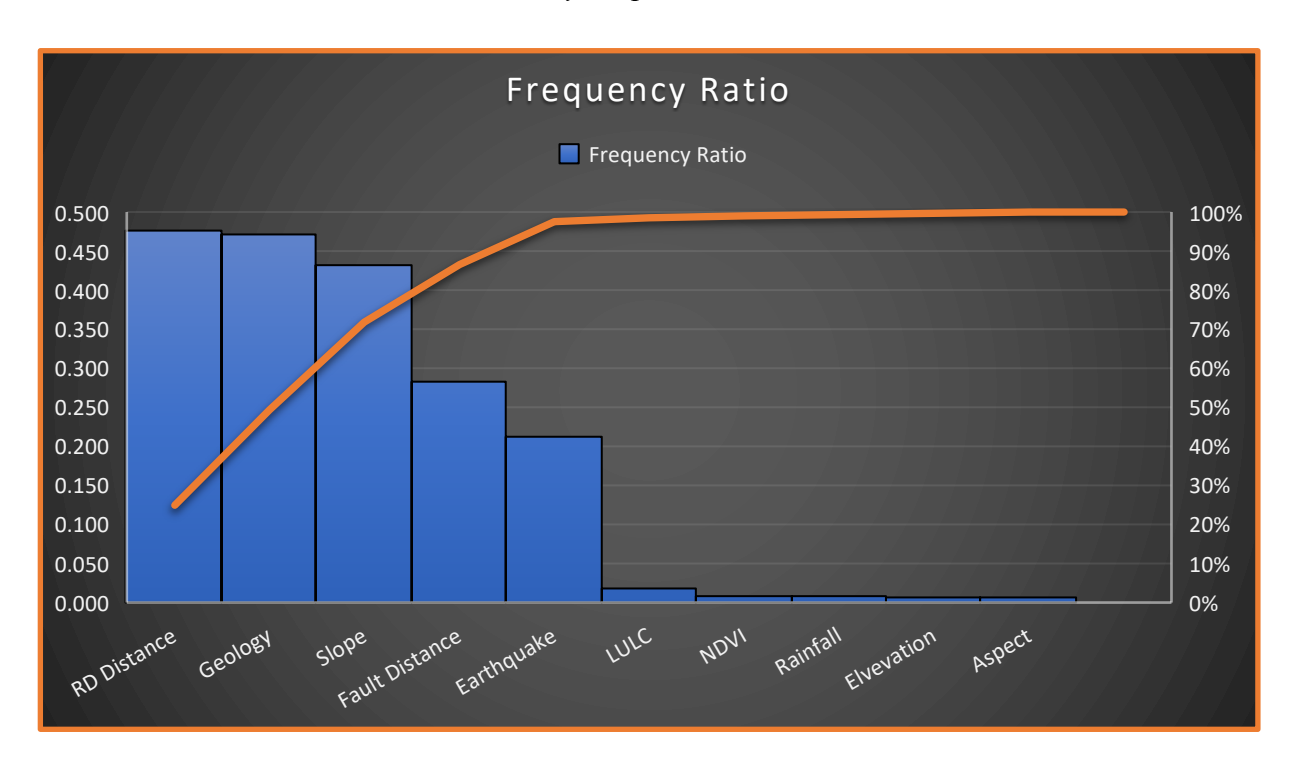


Figure 8: The frequency ratios of different landslide-related factors

Flood Extent in 2022 as Derived from SAR

A continuous rise in flooding was pragmatic in the inundation area from the Sentinel-1A data within 3 months since 13 March 2022 to 31 August 2022. In March, a significant percentage of the region was flooded under water owing to a particularly impacted exposure in Figure 10. Nevertheless, in later months, such as August of 2022, the extent of the flood inundation increased. The comparison between these months has been shown in the display figure that has been generated in the software ArcGIS 10.5 after applying the analysis of the normalized difference water index (NDWI). The difference in water bodies has been shown very clearly through magnificent results. The Indus River touches the borderline of Battagram, and some stream coverage in which the flood extends seems to be through image processing.

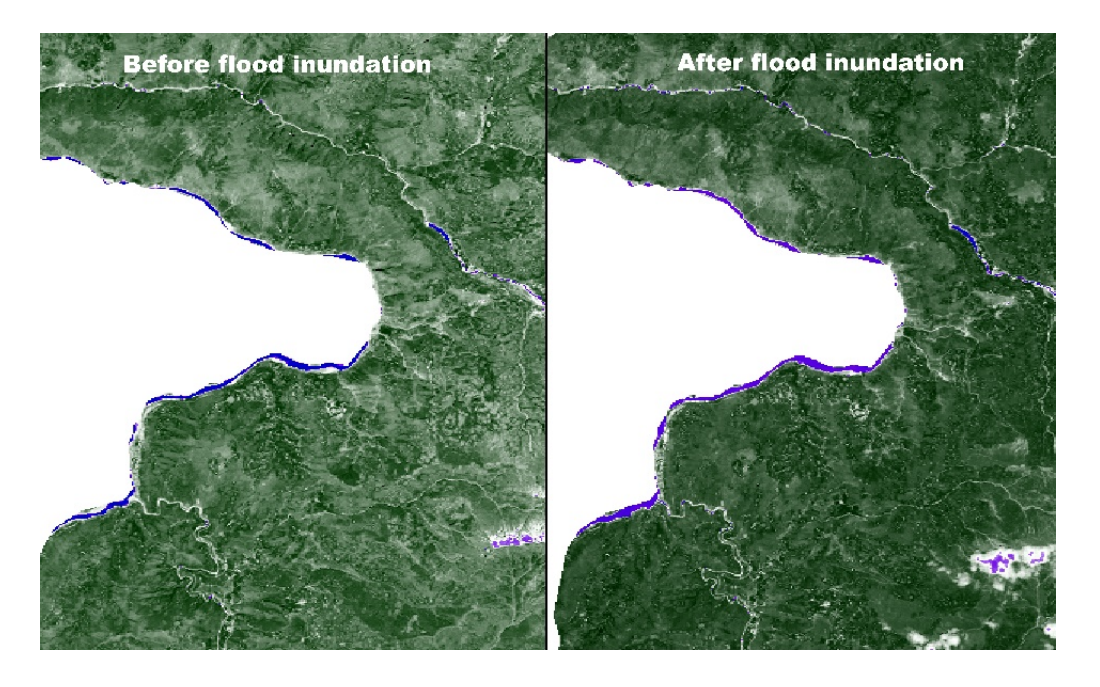


Figure 9: Comparison between before and after flood simulation

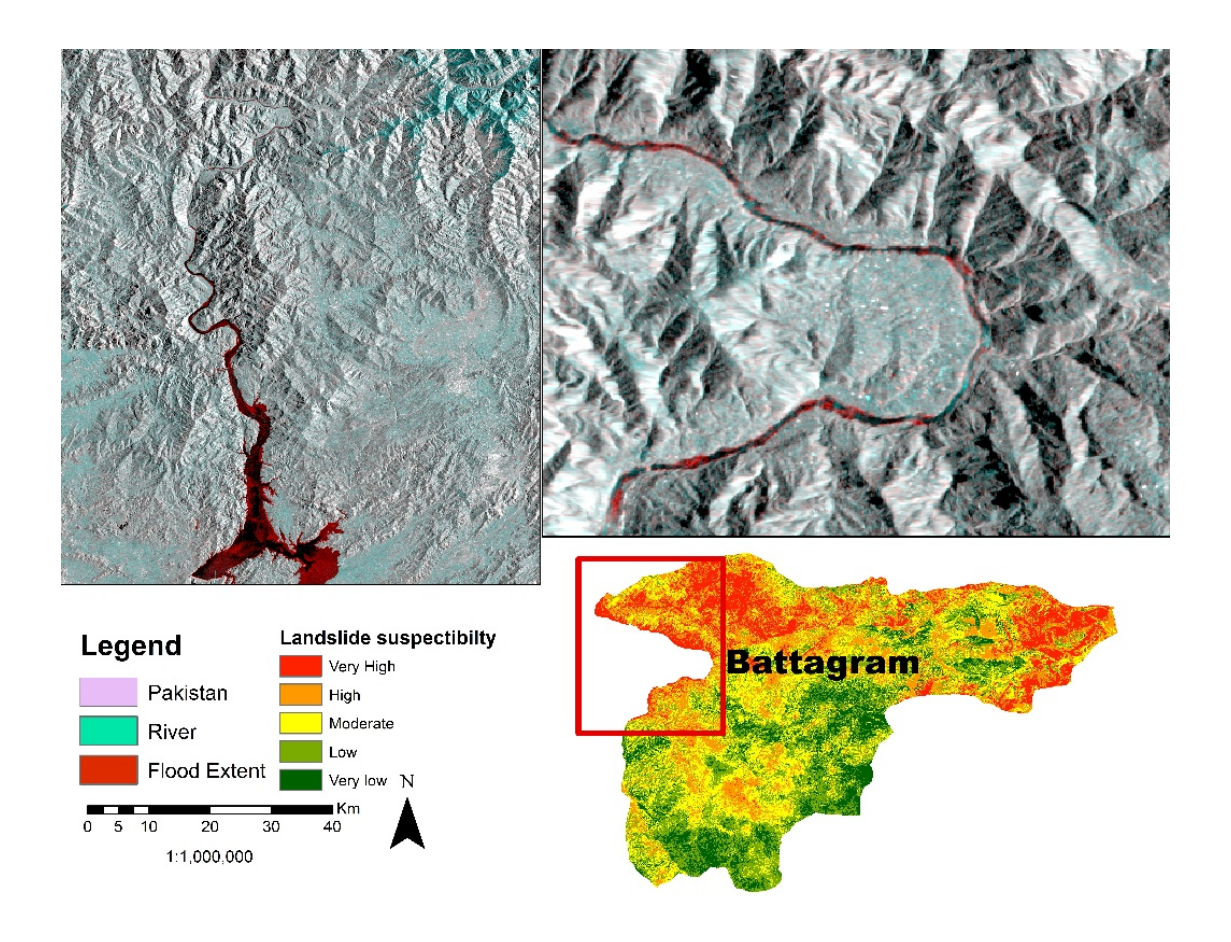


Figure 10: The flood extend map

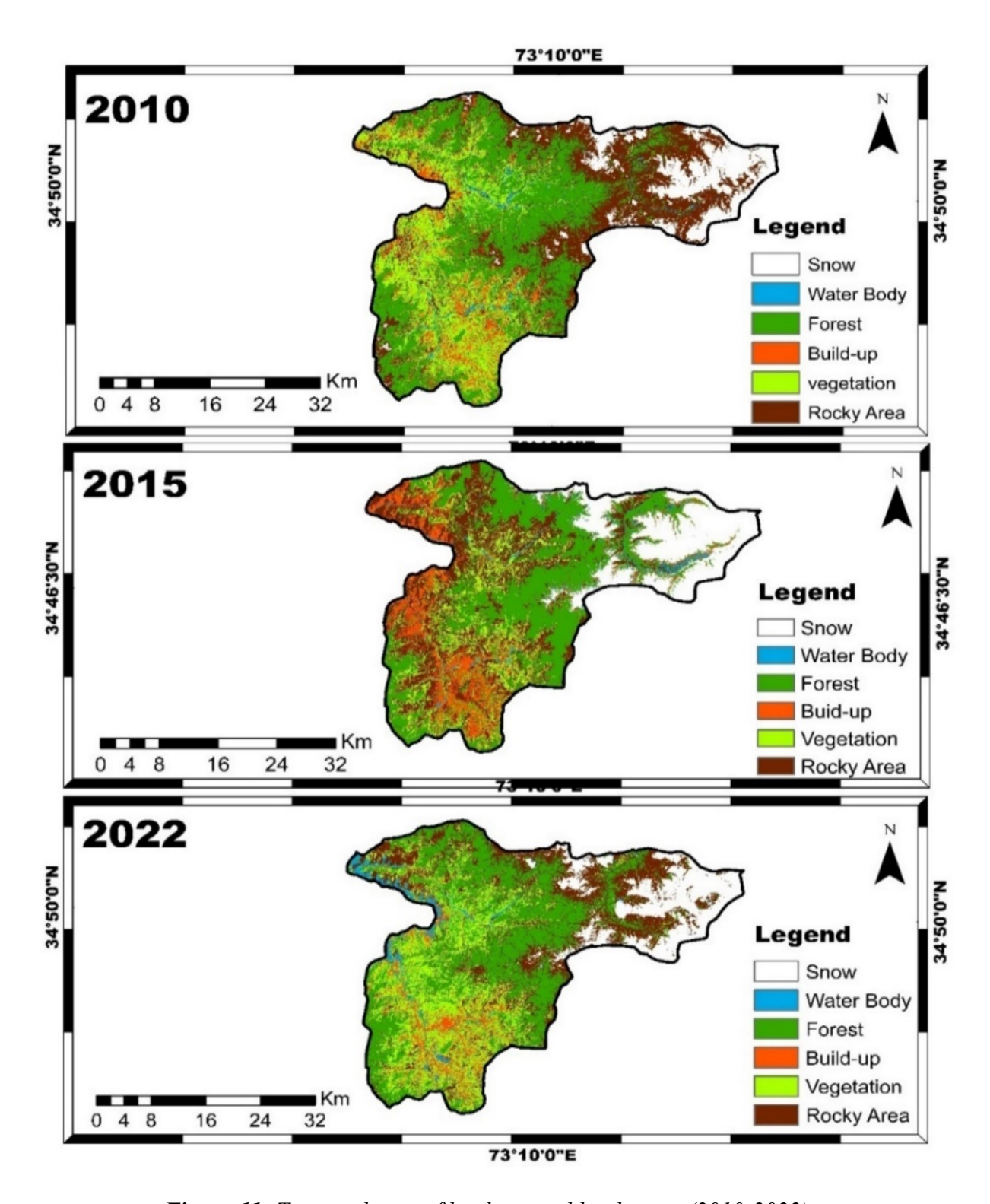


Figure 11: Temporal map of land use and land cover (2010-2022)

Figure 11. Presents the LULC changes by comparing categorized Landsat photos from 2010 and 2022. Significant increases were observed in the case of the water body, while major losses were observed in the forest. Although there was a minor increase in snow, the overall

amount of built-up contributing increased in 2015 to 11.85 then decreased due to flood, so the migration may be the reason of the declining rate of built-up. By using randomly selected samples that were spatially well-distributed, the total accuracy of the classification process was found to be 82.37%. Since our goal was to investigate agricultural land, the results were ultimately compared with LULC to mask out the permanent characteristics like forests and glaciers.

Table 2: The area calculation of LU/LC throughout 2010-2022

LULC results of the study area and comparison of both the years (2010–2022).						
Years	2010		2015		2022	
	Area(sq	Percentag	Area(sq	Percentag	Area(sq	Percentag
Classes	km)	e (%)	km)	e (%)	km)	e (%)
	1687.0					
Snow	6	11.27	2542.01	16.98	2051.09	13.7
Water Body	254.97	1.7	431.74	2.88	544.24	3.63
	4784.6					
Forest	1	31.96	4731.33	31.61	4818.3	31.19
Build-up	847.91	5.66	1774.36	11.85	809.89	5.41
	3062.9					
Vegetation	2	20.46	1731.58	11.56	3324	22.2
	4328.9					
Rocky area	7	28.92	3755.42	25.09	3418.92	22.84

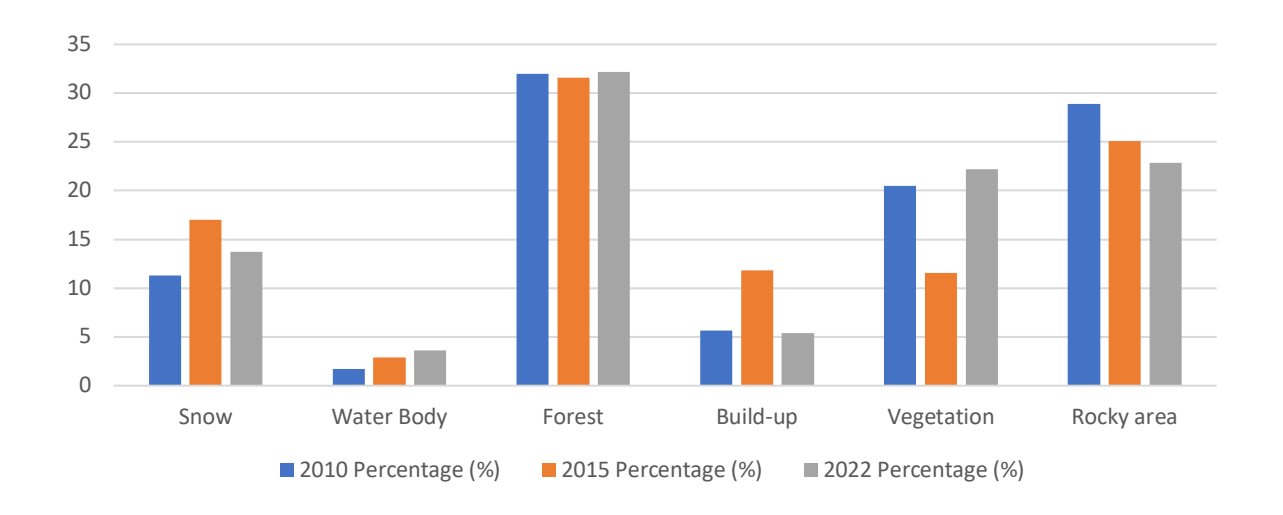


Figure 12: Graphical representation of landcover

Weighted Sum Analysis

These final weights are integrated into the GIS environment and used in ArcGIS software to generate the resulting map using the Weighted Sum method. Five classes have been generated from the results as shown in the map Very high (5.41%), high (42.5714%), moderate (36.0127%), low (14.2585%), and very low (1.74178%).

Table 3: The weights assigned to all factors

Data layer	Weight	
Aspect	3	
Slope (degree)	30	
Elevation(m)	11	
Rainfall	10	
Rd distance	5	
Fault distance	8	
Land use/land cover	8	
Geology	10	
Earthquake	10	
NDVI	5	

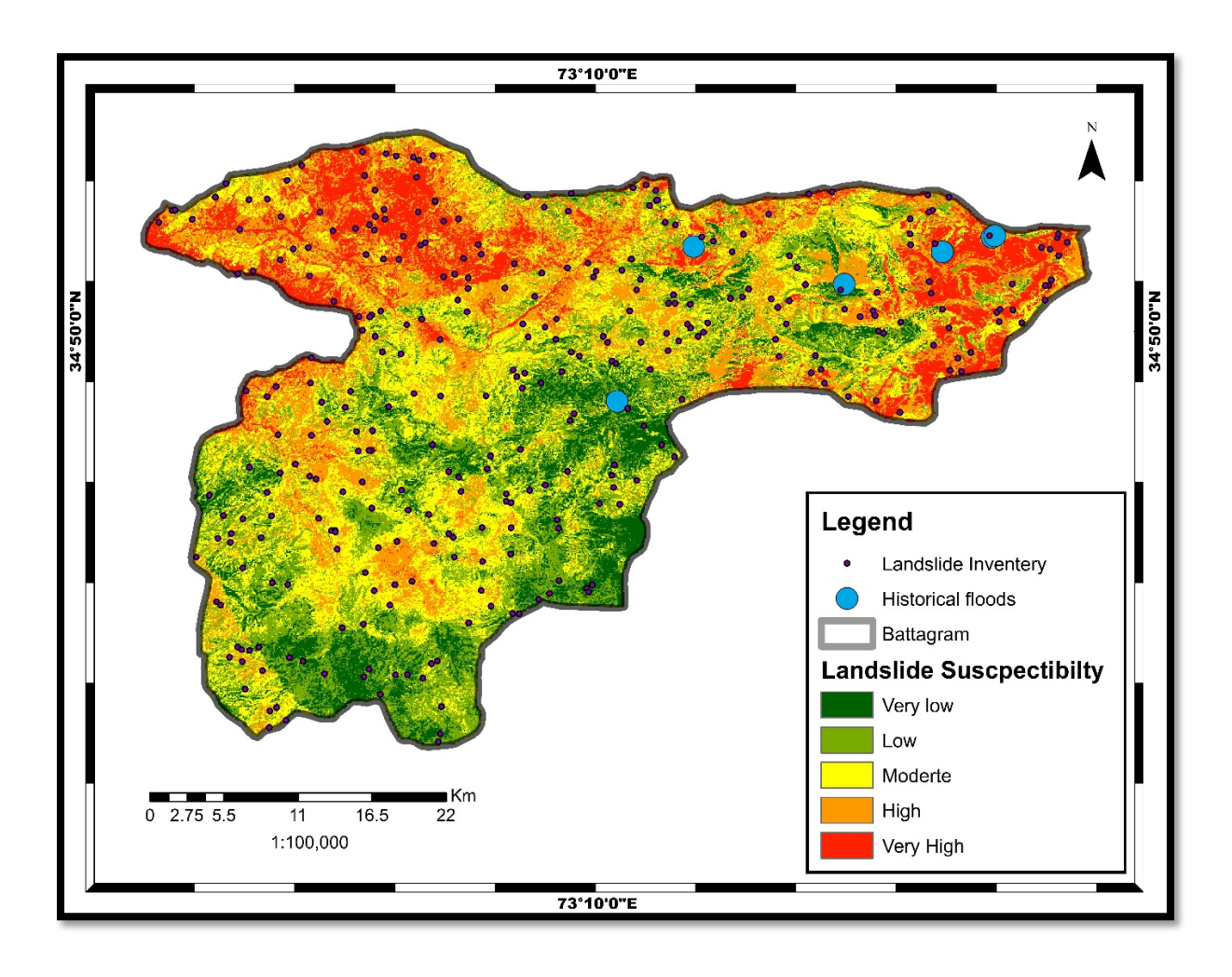


Figure 13: The landslide susceptibility map by using weighted sum analysis

Frequency ratio model

From the association between the landslide-causing factors and the places where landslides had not happened, one might infer the relationship between the landslide occurrence area and the landslide causal factors. A straightforward statistical method known as the frequency ratio approach has been used to determine the landslide susceptibility. To advance an LSM map, the frequency ratio for the designated contributing influence classes was mutual in geospatial (Figure 13).

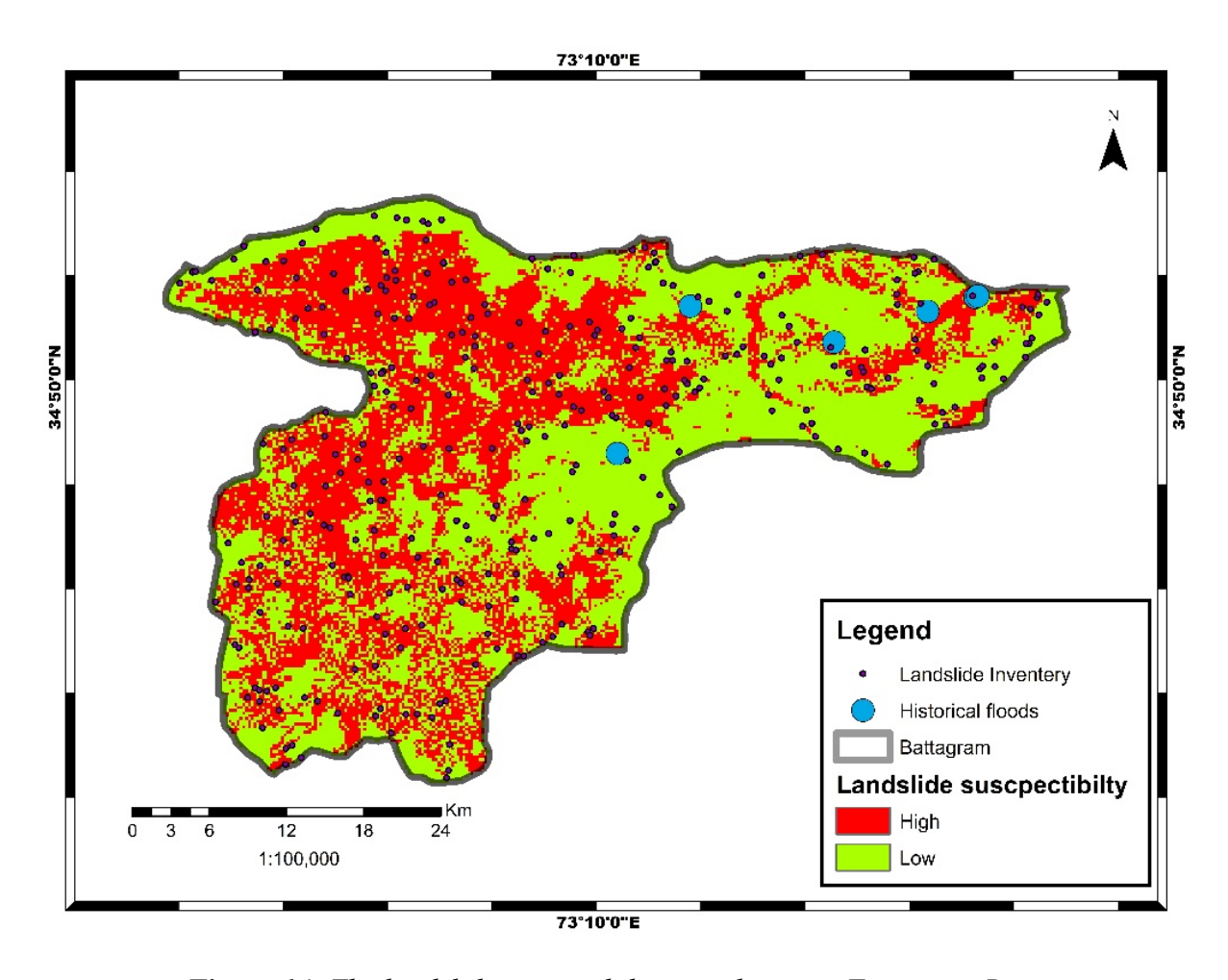


Figure 14: The landslide susceptibility map by using Frequency Ratio

Towards advance a landslide susceptibility map for learning zone, the LSM map is classed into two classes: very low and extremely high susceptibility (Fig. 15).

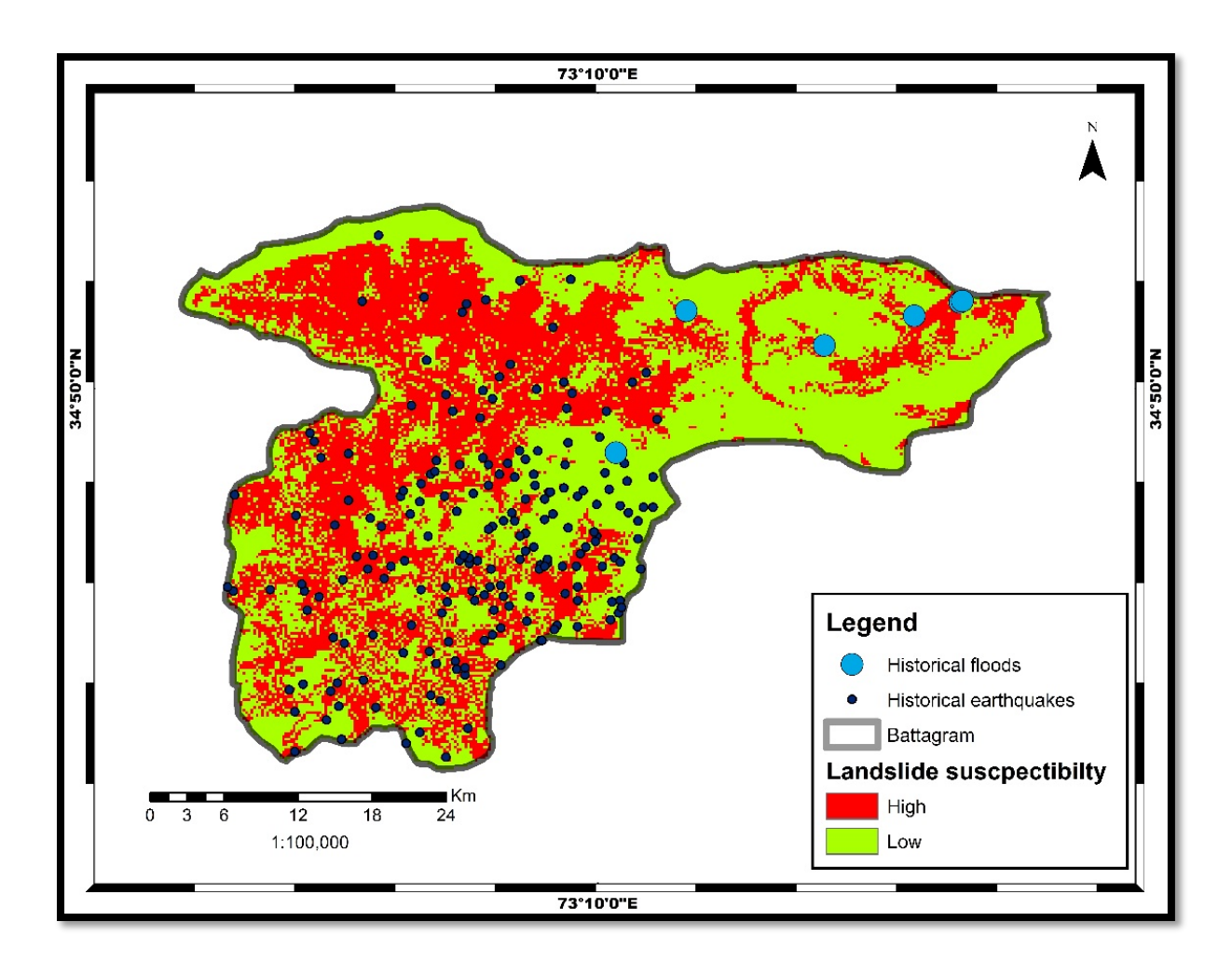


Figure 15: Landslide susceptibility map induced from earthquake and flood

According to the results, 44.67% of the range is in the very high class, followed by the high susceptibility class (40.94%), moderate class (11.61%), low susceptibility class (1.96%), and very low susceptibility class (0.79%). The LSM map (Fig. 15) gives rise to the success rate curve. The LSM map's index values for every pixel stayed as expected overall. The 1% cumulative intervals were used to reclassify these values into 100 classes. The landslide susceptibility map and the classified map used to overlap. According to the justification results, 70% of the pixels are correctly categorized as landslide pixels.

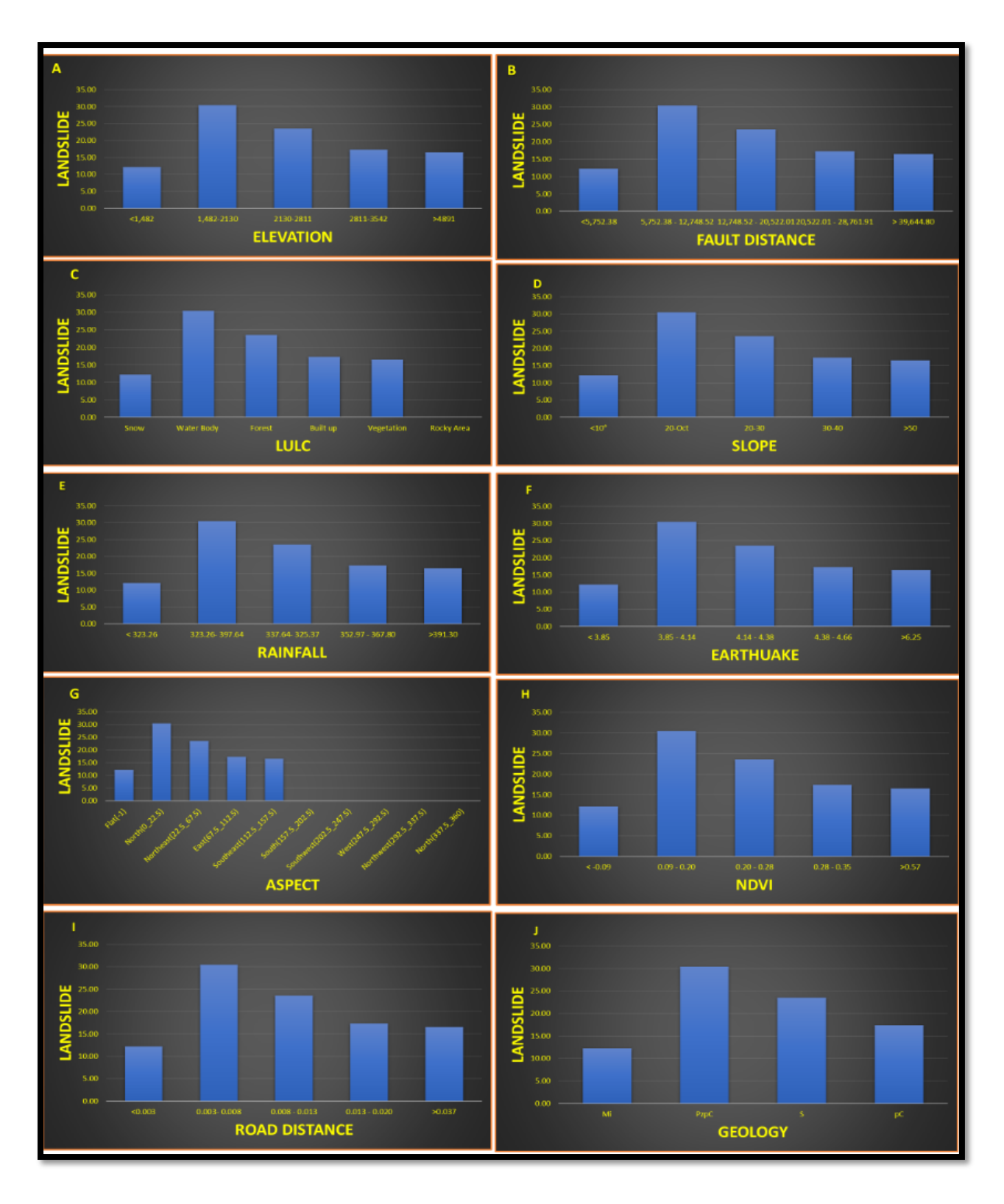


Figure 16: The Relationship between landslide and all parameters

Table 4: The calculation of frequency ratio for landslide susceptibility

Parameters	Class	Value	Class Pixcel	%Pixcel		landsliidng Pixe	FR
Elvevation	<1,482	1	381830	22.21	231	12.19	0.001
	1,482-2130 2130-2811	3	440629 348330	25.63 20.26	577 446	30.45 23.54	0.001 0.001
	2811-3542	4	311525	18.12	328	17.31	0.001
	>4891	5	237177	13.79	313	16.52	0.001
			1719491		1895		0.006
	<- 0.09	1	175123	11.70	231	12.19	0.001
	0.09 - 0.20	2	180965	12.09	577	30.45	0.003
NDVI	0.20 - 0.28	3	399932	26.72	446	23.54	0.001
	0.28 - 0.35	4	486289	32.49	328	17.31	0.001
	>0.57	5	254335	16.99	313	16.52	0.001
	< 73.99603642	1	1496644 314573	18.29	1895 231	12.19	0.008 0.001
	73.99 - 148.99	2	278285	16.18	577	30.45	0.002
	148.99- 216.91	3	376541	21.90	446	23.54	0.001
Aspect	216.91 - 287.66	4	352692	20.51	328	17.31	0.001
	> 359.82	5	397400	23.11	313	16.52	0.001
	- 555.52	Ť	1719491		1895	10.02	0.006
	<3.85	1	6919	14.05	231	12.19	0.033
	3.85 - 4.14	2	10190	20.69	577	30.45	0.057
	4.14 - 4.38	3	13978	28.39	446	23.54	0.032
Earthquake	4.38 - 4.66	4	13424	27.26	328	17.31	0.024
	> 6.25	5	4732	9.61	313	16.52	0.066
			49243		1895		0.212
	<5,752.38	1	10707	29.17	231	12.19	0.022
	5,752.38 - 12,748.52	2	9668	26.34	577	30.45	0.060
	12,748.52 - 20,522.01	3	6059	16.51	446	23.54	0.074
Fault Distance	20,522.01 - 28,761.91	4	6031	16.43	328	17.31	0.054
	> 39,644.80	5	4236	11.54	313	16.52	0.074
	7 33,044.00	_	36701	11.54	1895	10.52	0.283
	Snow	1	205109	13.70	231	12.19	0.001
	Water Body	2	54424	3.64	577	30.45	0.011
	Forest	3	481830	32.19	446	23.54	0.001
LULC	Built up	4	80989	5.41	328	17.31	0.004
LULC	Vegetation	5	332400	22.21	313	16.52	0.001
	Rocky Area	6	341892	22.84	1895	10.02	0.000
	Rocky Area	•		22.04	1093		
			1496644				0.018
	< 3.85	1	415847	27.71	231	12.19	0.001
	3.85 - 4.14	2	556394	37.07	577	30.45	0.001
Rainfall	4.14 - 4.38 4.38 - 4.66	3 4	216290	14.41	446	23.54	0.002
	4.38 - 4.66 >6.25	5	186865 125352	12.45 8.35	328 313	17.31 16.52	0.002 0.002
	- 5.25	Ť	1500748	- 0.00	1895	10.02	0.002
	<0.003	1	24328	49.40	231	12.19	0.009
	0.003- 0.008	2	13073	26.55	577	30.45	0.044
RD Distance	0.008 - 0.013	3	7080	14.38	446	23.54	0.063
	0.013 - 0.020	4	3596	7.30	328	17.31	0.091
	>0.037	5	1166 49243	2.37	313 1895	16.52	0.268 0.476
	<10°	1	49243	65.46	231	12.19	0.476
	20-Oct	2	251548	33.29	577	30.45	0.000
Slope	20-30	3	5765	0.76	446	23.54	0.077
	30-40	4	1994	0.26	328	17.31	0.164
	>50	5	1666	0.22	313	16.52	0.188
			755572		1895		0.432
Castani	Mi	1	11381	21.95	231	12.19	0.020
	PzpC	2	1408	2.72	577	30.45	0.410
Geology	S	3 4	17065	32.92	446 328	23.54	0.026
	рС	4	21990 51844	42.42	328 1582	17.31	0.015 0.471
			0.077		1002	I.	U77 I

The landslide susceptibility map comprises of the predicted landslide area hence it can be used to decrease the potential hazard associated with the landslides in this study area. It means this model is 88.9% accurate to predict the probability of landslide and the model is 92.3% success to generate the prediction in the study area.

Table 5: The prediction ratio for all the factors

Slope (degree)	2.357866	235.79		
Elevation(m)	2.17186737	217.19		
Rainfall	1.03679384	103.68		
Rd distance	2.95838643	295.84		
Fault distance	1	100.00		
induse/land cov	3.24558626	324.56		
Geology	4.56060049	456.06		
Earthquake	1.06810309	106.81		
NDVI	1.8171733	181.72		



Figure 17: Graphical representation of Prediction ratio

Conclusion

The purpose of this work was to create a complete database of landslides caused by the Battgaram earthquake and rainfall by interpreting multitemporal images and correlating them with environmental, seismic, and rainfall parameters. These landslides resulted from a mix of rainfall- and earthquake-induced occurrences. It is difficult to assess how the climate affects landslides because the two phenomena only partially overlap in space and time. While rainfall

is likely the most frequent cause of landslides, this study has identified earthquakes and floods as additional triggers for landslide risk. The northern portion of Battgaram is closely watching the extent of the flood and the activation of the earthquake in 2022, which increases the susceptibility of landslides. Examining the landslide inventory map made especially for the study area, it is evident that the majority of the region's active landslide locations are located in its higher-elevation sections. The findings lead to the following conclusions, which are proposed: The purpose of this study was to use geographic methods to create an LSM of the research region in order to lessen the effects of potential dangers. The weighted sum analysis of the study showed that 1.74178% of the area had very low susceptibility. The area of Muzaffarabad is divided into four susceptibility zones: high (2.5714%), moderate (36.0127%), low (14.2585%), and very high (5.41%). Specifically, 44.67% of the range falls into the very high class, followed by the high susceptibility class (40.94%), the moderate class (11.61%), the low susceptibility class (1.96%), and the very low susceptibility class (0.79%) in the frequency ratio model. In the current study, the GIS-based statistical models WSM and FR were utilized to calculate the correlation between dependent variables (the elements that cause landslides) and dependent variables (the events or inventories of landslides).

The purpose of this study was to assess the relationship between the occurrence of landslides and causal factors. The topography, geology, hydrology, climate, and geomorphology of these factors were listed. After applying the Weight Sum analysis method and transferring the weight data to the GIS environment, a landslide susceptibility map was produced. The results of the validation showed that the FR model is a reliable approach for the LSM. The susceptibility map was validated by comparing its positions with those of known landslides. 85.7% of the predictions were shown to be accurate. We conclude that the most authentic, adaptable, and dependable way to generate LSM is through statistical modeling based on GIS. The maps of landslide susceptibility that this study produced are crucial for local governance and sustainable urban development. Initial decision-making and policy planning may benefit from the data obtained from the created map. Furthermore, in order to be widely applied in more regional areas, more relative data must be obtained.

Acknowledgment

I am appreciative of my parents and Mr. Saddam Hussain Research Associate at Government College University Lahore, for his help and encouragement with the technical aspects of the job.

References

- Abdı, A., Bouamrane, A., Karech, T., Dahri, N., & Kaouachi, A. (2021). Landslide Susceptibility Mapping Using GIS-based Fuzzy Logic and the Analytical Hierarchical Processes Approach: A Case Study in Constantine (North-East Algeria). *Geotechnical and Geological Engineering*, 39(8), 5675–5691. https://doi.org/10.1007/s10706-021-01855-3
- Bahram, I., & R. Paradise, T. (2020). Seismic Risk Perception Assessment of Earthquake Survivors: A Case Study from the 2005 Kashmir Earthquake. *Open Journal of Earthquake Research*, 09(05), 403–416. https://doi.org/10.4236/ojer.2020.95023
- Bali, B. S., Wani, A. A., Mir, S. A., Irfan, M., & Farooq, D. (2025). Rupture length as a proxy for quantifying palaeo-earthquake magnitude for future seismic micro-zonation in Kashmir, NW Himalaya, India. *Natural Hazards*. https://doi.org/10.1007/s11069-025-07189-0
- Batar, A. K., & Watanabe, T. (2021). Landslide Susceptibility Mapping and Assessment Using Geospatial Platforms and Weights of Evidence (WoE) Method in the Indian Himalayan Region: Recent Developments, Gaps, and Future Directions. *ISPRS International Journal of Geo-Information*, 10(3), 114. https://doi.org/10.3390/ijgi10030114
- Camilo, D. C., Lombardo, L., Mai, P. M., Dou, J., & Huser, R. (2017). Handling high predictor dimensionality in slope-unit-based landslide susceptibility models through LASSO-penalized Generalized Linear Model. *Environmental Modelling and Software*, 97, 145–156. https://doi.org/10.1016/j.envsoft.2017.08.003
- Chen, L., Guo, Z., Yin, K., Pikha Shrestha, D., & Jin, S. (2019). The influence of land use and land cover change on landslide susceptibility: A case study in Zhushan Town, Xuan'en County (Hubei, China). *Natural Hazards and Earth System Sciences*, 19(10), 2207–2228. https://doi.org/10.5194/nhess-19-2207-2019
- Dahiya, N., Pandit, K., Sarkar, S., & Pain, A. (2025). Various Aspects of Rockfall Hazards along the Mountain Roads in India: A Systematic Review. *Indian Geotechnical Journal*, 55(3), 2007–2029. https://doi.org/10.1007/s40098-024-01015-3
- Dietrich, A. M., Müller, G. J., & Schoenle, R. S. (2024). Big news: Climate-disaster expectations and the business cycle. *Journal of Economic Behavior & Organization*, 227, 106719. https://doi.org/10.1016/j.jebo.2024.106719
- Duan, Y., Luo, J., Pei, X., & Liu, Z. (2023). Co-Seismic Landslides Triggered by the 2014 Mw 6.2 Ludian Earthquake, Yunnan, China: Spatial Distribution, Directional Effect, and Controlling Factors. *Remote Sensing*, *15*(18), 4444. https://doi.org/10.3390/rs15184444
- Hussain, M. A., Shuai, Z., Moawwez, M. A., Umar, T., Iqbal, M. R., Kamran, M., & Muneer, M. (2023). A Review of Spatial Variations of Multiple Natural Hazards and Risk Management Strategies in Pakistan. *Water*, 15(3), 407. https://doi.org/10.3390/w15030407
- Hussen, H. M., Chala, E. T., & Jilo, N. Z. (2024). Slope stability analysis of colluvial deposits along the Muketuri-Alem Ketema Road, Northern Ethiopia. *Quaternary Science Advances*, 16, 100239. https://doi.org/10.1016/j.qsa.2024.100239
- Jena, R., Pradhan, B., Naik, S. P., & Alamri, A. M. (2021). Earthquake risk assessment in NE India using deep learning and geospatial analysis. *Geoscience Frontiers*, 12(3), 101110–101110. https://doi.org/10.1016/j.gsf.2020.11.007
- Jin, H., Huang, L., Wang, C., Li, C., Yizi, H., Bai, Z., Sun, L., Zhao, Z., Chen, B., & Liu, Y. (2024). Induced pattern of high and steep slope landslides under rainfall conditions. *Journal of Geophysics and Engineering*, 21(1), 142–154. https://doi.org/10.1093/jge/gxad098

- Khan, H., Shafique, M., Khan, M. A., Bacha, M. A., Shah, S. U., & Calligaris, C. (2019a). Landslide susceptibility assessment using Frequency Ratio, a case study of northern Pakistan. *Egyptian Journal of Remote Sensing and Space Science*, 22(1), 11–24. https://doi.org/10.1016/j.ejrs.2018.03.004
- Khan, H., Shafique, M., Khan, M. A., Bacha, M. A., Shah, S. U., & Calligaris, C. (2019b). Landslide susceptibility assessment using Frequency Ratio, a case study of northern Pakistan. *Egyptian Journal of Remote Sensing and Space Science*, 22(1), 11–24. https://doi.org/10.1016/j.ejrs.2018.03.004
- Konurhan, Z., Yucesan, M., & Gul, M. (2023). Integrating stratified best–worst method and GIS for landslide susceptibility assessment: A case study in Erzurum province (Turkey). *Environmental Science and Pollution Research*, *30*(53), 113978–114000. https://doi.org/10.1007/s11356-023-30200-9
- Linkha, T. R. (2024). Landslide and flood disaster: Causes and its responses. *Journal of Population and Development*, *5*(1), 188–202. https://doi.org/10.3126/jpd.v5i1.67577
- Lu, H., Li, W., Xu, Q., Yu, W., Zhou, S., Li, Z., Zhan, W., Li, W., Xu, S., Zhang, P., Dong, X., Liang, J., & Ge, D. (2024). Active landslide detection using integrated remote sensing technologies for a wide region and multiple stages: A case study in southwestern China. *Science of The Total Environment*, *931*, 172709. https://doi.org/10.1016/j.scitotenv.2024.172709
- Mir, R. A., Habib, Z., Kumar, A., & Bhat, N. A. (2024). Landslide susceptibility mapping and risk assessment using total estimated susceptibility values along NH44 in Jammu and Kashmir, Western Himalaya. *Natural Hazards*, *120*(5), 4257–4296. https://doi.org/10.1007/s11069-023-06363-6
- Munir, B. A., Ahmad, S. R., & Rehan, R. (2021). Torrential Flood Water Management: Rainwater Harvesting through Relation Based Dam Suitability Analysis and Quantification of Erosion Potential. *ISPRS International Journal of Geo-Information*, 10(1), 27. https://doi.org/10.3390/ijgi10010027
- NASA. (2022). *Heatwaves and Fires Scorch Europe, Africa, and Asia*. https://earthobservatory.nasa.gov/images/150083/heatwaves-and-firesscorch-europe-africa-and-asia
- Rahim, I., Ali, S. M., & Aslam, M. (2018). GIS Based Landslide Susceptibility Mapping with Application of Analytical Hierarchy Process in District Ghizer, Gilgit Baltistan Pakistan. *Journal of Geoscience and Environment Protection*, 06(02), 34–49. https://doi.org/10.4236/gep.2018.62003
- Rehman, A., Song, J., Haq, F., Mahmood, S., Ahamad, M. I., Basharat, M., Sajid, M., & Mehmood, M. S. (2022). Multi-Hazard Susceptibility Assessment Using the Analytical Hierarchy Process and Frequency Ratio Techniques in the Northwest Himalayas, Pakistan. *Remote Sensing*, *14*(3), 1–31. https://doi.org/10.3390/rs14030554
- Saima Akbar. (2024). Landslide Hazard Assessment of Kashmir. *Advances in Earth and Environmental Science*. https://doi.org/10.47485/2766-2624.1048
- Sana, E., Kumar, A., Robson, E., Prasanna, R., Kala, U., & Toll, D. G. (2024). Preliminary assessment of series of landslides and related damage by heavy rainfall in Himachal Pradesh, India, during July 2023. *Landslides*, *21*(4), 919–931. https://doi.org/10.1007/s10346-023-02209-1
- Schlögel, R., Marchesini, I., Alvioli, M., Reichenbach, P., Rossi, M., & Malet, J. P. (2018). Optimizing landslide susceptibility zonation: Effects of DEM spatial resolution and slope unit delineation on logistic regression models. *Geomorphology*, 301, 10–20. https://doi.org/10.1016/j.geomorph.2017.10.018

- Shabbir, W., Omer, T., & Pilz, J. (2023). The impact of environmental change on landslides, fatal landslides, and their triggers in Pakistan (2003–2019). *Environmental Science and Pollution Research*, 30(12), 33819–33832. https://doi.org/10.1007/s11356-022-24291-z
- Tyagi, A., Tiwari, R. K., & James, N. (2023). Mapping the landslide susceptibility considering future land-use land-cover scenario. *Landslides*, 20(1), 65–76. https://doi.org/10.1007/s10346-022-01968-7
- Vasil Levski, & Dolchinkov, N. T. (2024). Natural Emergencies and Some Causes of Their Occurrence: A Review. *Trends in Ecological and Indoor Environmental Engineering*, 2(1), 18–27. https://doi.org/10.62622/TEIEE.024.2.1.18-27
- Zou, S., Abuduwaili, J., Duan, W., Ding, J., De Maeyer, P., Van De Voorde, T., & Ma, L. (2021). Attribution of changes in the trend and temporal non-uniformity of extreme precipitation events in Central Asia. *Scientific Reports*, *11*(1), 1–11. https://doi.org/10.1038/s41598-021-94486-w

Received: 08 April 2025 Revision Received: 27 May 2025